VIII-Ⅱ-1. Project Research

Project 2

PR2 Application Studies on Effective Use of F-Elements

H. Yamana

Research Reactor Institute, Kyoto University

1. Objectives and Allotted Research Subjects

Studies on actinide nuclides with careful management are being more important for reprocessing, disposal, partitioning, and transmutation processes in the nuclear fuel cycle. Hot laboratory of KURRI is one of core facilities in Japan, in which actinides especially transuranic elements (Pu, Am, Cm, and so on) can be treated. In our series of past research projects, separation, purification, and synthesis procedures were found to be effective for other elements, for example, rare metal refining. In this context, the actinide studies are expanded for fundamental and application studies on f-elements. Allotted research subjects are as the followings.

ARS-1 Molecular dynamics simulation of molten salts containing f-elements (N. Ohtori *et al*.)

ARS-2 Spectroelectrochemical analysis of actinide ions in molten salts and hydrate melts (A. Uehara *et al.*)

ARS-3 XAFS analysis on halogenides containing actinides and FP elements (H. Matsuura *et al*.).

ARS-4 Study on chemical isotope effect of actinides and fission product elements (T. Fujii *et al.*).

ARS-5 Systematic study on bonding characteristics of trivalent actinides with ligands (A. Shinohara *et al*.).

ARS-6 Study on neutron capture cross sections of long-lived nuclides by activation method (S. Nakamura *et al*.).

ARS-7 Fundamental and application studies on effective use of f-elements (Y. Ikeda *et al*.).

ARS-8 Study on complexation of actinides in aqueous solutions (T. Sasaki *et al*.).

ARS-9 Electrochemical study of uranium in pyrochemical reprocessing system (Y. Sakamura *et al.*).

ARS-10 Fundamental study on electrolytic formation/dissolution of f-element compounds in molten salts (T. Goto *et al*.).

ARS-11 Absorption spectrophotometric study on titanium in molten salts. (H. Sekimoto *et al*.)

ARS-12 Thermal and mechanical properties of actinides-containing ceramics (S. Yamanaka *et al*.)

2. Main Results and Contents

ARS-1 and 7 studied the U chemistry in low temperature or room temperature melts. ARS-1 studied MD simulation for concentrated LiCl aqueous solutions containing uranyl chloride, and evaluated the local structure of U. In ARS-7, the electrochemical behavior of $(EMI)_2UO_2Cl_4$ (EMI: 1-ethyl-3-methylimidazoliun), in the mixture of EMICl and $EMIBF_4$ was studied and the basic data were obtained. ARS-2, 3, 9, 10, and 11 studied the chemical behavior of actinides, lanthanides, FP elements, and structural material elements in molten salts, the results of which are to be dedicated to the development of nuclear fuel cycle or general industrial use. ARS-2 studied electrochemical characteristics of Am in micro litter order volume of molten LiCl-RbCl eutectic. This is a first trial for using visible amount of Am in high temperature melt at KURRI. In ARS-3 and ARS-11, the electron absorption spectra of Nd were measured. Effects of adding fluoride or borate were clarified. ARS-9 studied reduction behavior of UCl_3 on Ni and Al electrodes in LiCl-KCl eutectic salt bath by cyclic voltammetry. Separation of U from Al was discussed. ARS-10 studied electrochemical behavior and liquid structures of molten alkaline chlorides containing Al. Raman spectra obtained were interpreted by using *ab initio* method. ARS-4, 5, and 8 studied aqueous chemistry of actinides and FP elements. ARS-4 studied Pd complexation by *ab initio* method. Optimized geometries of aqua- and chloro- Pd species were calculated. ARS-5 studied solvent extraction of ^{99}Mo. Carrier-free ^{99}Mo obtained from a Kyoto University Reactor (KUR) multitracer was used. ARS-8 studied the temperature effect of Th solubility. The Th solublity at 363 K was clarified. Nuclear physical properties of TRUs were investigated in the study, ARS-6. By activation method using KUR, the thermal-neutron capture cross section of ^{243}Am was newly evaluated. In ARS-9, polycrystalline samples of Y_6UO_{12} were synthesized by solid state reactions. XRD, SEM, and EDX data were successfully obtained.

3. Summaries of the achievements

In this research, by using various unique facilities of KURRI for f-element research, new and characteristic chemical and nuclear physical data were obtained. These new information encompass solid chemistry, molten salt and solution chemistry, as well as nuclear reactions of f-elements. The results are useful either for scientific purpose or for technological purpose for nuclear science and general industry.

採択課題番号 24P2　　ｆ－元素の有効利用に関わる基礎及び応用研究　　プロジェクト
（京大・原子炉）山名　元

PR2-1 Local Structure around Uranyl Ion in Concentrated LiCl Aqueous Solutions

N. Ohtori, Y. Ishii, Y. Nagata, A. Uehara[1], T. Fujii[1], H. Yamana[1], K. Minato[2] and Y. Okamoto[2]

Department of Chemistry, Niigata University
[1]Research Reactor Institute, Kyoto University
[2]Japan Atomic Energy Agency

INTRODUCTION: Electrochemical property of uranyl ion in aqueous solution highly concentrated by LiCl is significantly different from that in the dilute solutions, and similar to that in the molten salt [1]. These highly concentrated aqueous solutions are considered for the electrolyte medium in the dry reprocessing of spent nuclear fuels, instead of high temperature molten salts. Recent experimental works [2,3] reveal that the local structure around uranyl ion in the concentrated solutions is intermediate between the dilute solutions and molten salts. On the other hands, there is no report on the local structure in such concentrated solutions using simulation techniques. In the present work, we have performed molecular dynamics (MD) simulation for LiCl aqueous solutions containing uranyl chloride, and evaluated the local structure in the highly concentrated solution.

CALCULATIONS: All the MD calculations have been carried out with *NVE* ensemble. The time step was 1.0 fs. The SPC/E model was used for water molecule, and the other ion models were cited from ref [4,5]. The water and uranyl molecules were treated as rigid bodies with SHAKE method. The LiCl concentration was set at 0, 1, 3, 5, 8, 14 M, and the concentration of uranyl chloride consistently at 0.05 M. After equilibrating the systems at 298 K, we evaluated the self-diffusion coefficient, radial distribution function, angular distribution function, and coordination number distribution in each solution. In 14M LiCl, the U L_{III}-edge extended X-ray absorption fine structure (EXAFS) spectrum was theoretically calculated using the FEFF code [6].

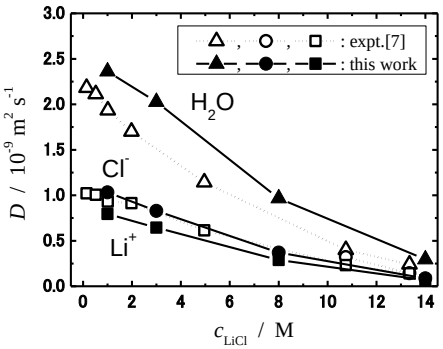

Fig.1 Self-diffusion coefficients in LiCl aqueous solutions.

RESULTS: Figure 1 shows the self-diffusion coefficients in each solution. The calculated results are in good agreements with the experimental result [7] for a whole range of concentration. However, as shown in table.1, the U-Cl distance and coordination numbers in 14M LiCl are underestimated compared with the experimental results [3]. Figure 2 shows the Fourier transforms of experimental[3] and calculated EXAFS spectra. The calculated U-Cl correlation shows very lower and more distance than the experimental result [3]. These disagreements of the local structure should be traceable to the insufficient interatomic potential between uranyl ion and Cl ion.

Table.1 Coordination distances and numbers for uranyl ion in 14 M LiCl.

	U-OH_2		U-Cl	
	r / Å	*N*	*r* / Å	*N*
expt.[3]	2.47	1.3	2.73	2.4
this work	2.50	4	2.94	1

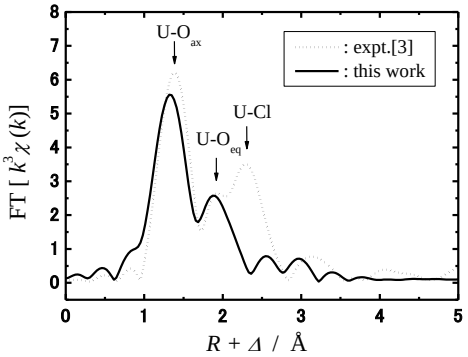

Fig.2 Fourier transforms of experimental and calculated U L_{III}-edge EXAFS spectra in 14M LiCl.

REFERENCES:

[1] A. Uehara, O. Shirai, T. Fujii, T. Nagai and H. Yamana, *J. Appl. Electrochem.*, **42**, 455(2012).
[2] P. Allen, J. Bucher, D. Shuh, N. Edelstein and T. Reich, *Inorg. Chem.*, **36**, 4676(1997).
[3] A. Uehara, T. Fujii, H. Matsuura, N. Sato, H. Yamana and Y. Okamoto, *OECD-NEA*, **15**, 197(2009).
[4] J. Greathouse, R. O'Brien, G. Bemis and R. Pabalan, *J. Phys. Chem. B*, **106**, 1646(2002).
[5] S. H. Lee and J. C. Rasaiah, *J. Phys. Chem.*, **100**, 1420(1996).
[6] A. L. Aukudinov, B. Ravel, J. J. Rehr and S. D. Conradson, *Phys. Rev. B*, **58**, 7565(1998).
[7] K. Tanaka and M. Nomura, *J. Chem. Soc. Faraday Trans.*, 1, **83**, 1779(1987).

採択課題番号 24P2-1　融体中での f-元素の分子動力学計算と実験系の照合研究　プロジェクト（新潟大・理）大鳥範和、石井良樹、永田優太（京大・原子炉）上原章寛、藤井俊行、山名　元（JAEA）湊　和生、岡本芳浩

PR2-2 Electrochemical Measurement of Americium Ion in 0.1 ml Solution of High Temperature Molten LiCl-RbCl Eutectic

A. Uehara, T. Nagai[1], T. Fujii, K. Fukasawa[2], T. Uda[2] and H. Yamana

Research Reactor Institute, Kyoto University
[1]Nuclear Fuel Cycle Engineering Lab., Japan Atomic Energy Agency
[2]Graduate School of Engineering, Kyoto University

INTRODUCTION:

In currently proposed aqueous separation systems, in which dedicated extractants are used to extract trivalent actinides from High Active Waste (HAW), co-recovery of Am and Cm is possible. However, a large separation process, which is necessary for the removal of lanthanides from trivalent MAs, spoils the cost efficiency, and it is practically impossible to separate Am from Cm. Even in a pyrochemical reprocessing system, which is based upon an electro-refining technique using molten salt, Am/Cm separation is very difficult, because their standard redox potentials are very close. In this context, this paper focuses attention to the possibility of Am isolation utilizing the divalency of Am, which can exist in molten chloride melt. In the present report, we studied electrochemical characteristics of Am in micro litter order volume of molten LiCl-RbCl eutectic

EXPERIMENTAL:

Solid Am oxide was dissolved into nitric acid and heated. The solid $Am(NO_3)_3$ after drying up was dissolved into LiCl-RbCl (55:45) eutectic melt at 773 K. $Am(NO_3)_3$ was converted to $AmCl_3$ by purging Cl_2 gas into the melt. In the electrochemical measurements, about 0.015 mol% $AmCl_3$ solutions of molten LiCl-RbCl was used. PYREX glass membrane tube of 3 mm inner diameter was used for the measurement. A 0.6 mmϕ tungsten wire was used for working and counter electrode, both covered with alumina sheath (Fig. 1).

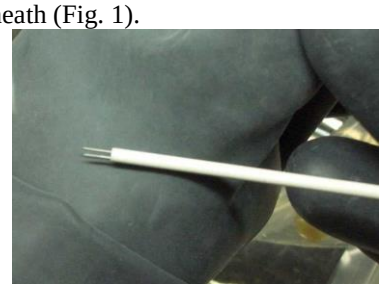

Fig.1 Working and counter electrodes (0.6 mmϕ tungsten wire).

An $Ag|Ag^+$ reference electrode composed with an Ag wire|1 mol% AgCl in a bulk melt|PYREX glass membrane tube was used. Those two glass membrane electrodes were inserted into bulk LiCl-RbCl melt. Electrochemical measurement system HZ-5000 (Hokuto-Denko Co. Ltd.) was used for the voltammetry measurements. All the experiments were carried out in a glove box filled with dry argon whose humidity and oxygen impurity was continuously kept less than 1 ppm.

RESULTS:

100 µl of sample solution ([Am] = 0.14 mol%) was used for electrochemical measurements. Open circuit potential (E_{OCP}) was monitored to estimate dissolving ions determining the equilibrium potential in the solution. Here, the equilibrium potential is depended on concentration and oxidation state of ions dissolving in the melt. E_{OCP} showed -1.08 V vs. Cl/Cl_2 which was positive enough to the redox potential of Am. It has been reported that the electrochemical of Am ion is similar to that of Nd as follows[1];

$$Am^{3+} + e^- \rightarrow Am^{2+} \quad (1)$$

Furthermore, generated Am^{2+} disproportionates to form Am^{3+} and metallic Am,

$$3\,Am^{2+} \rightleftarrows 2\,Am^{3+} + Am^{(0)} \quad (2)$$

In order to study electrochemical behaviour of Am in molten LiCl-RbCl eutectic, differential pulse voltammogram was measured. Three reduction peaks at -1.78, -2.12 and -2.90 V were observed. The peak at -2.90 V seems to be close to the reduction potential of the $Am^{3+}|Am^{(0)}$ couple, which is calculated based on the redox potential of the $Am^{3+}|Am^{(0)}$ couple in LiCl-KCl eutectic[2] and averaged polarizing power of the LiCl-RbCl eutectic [3]. Here, the redox potential was assumed to show linear dependence on the averaged polarizing power of component cations of solvent melt consisted of the mole fraction, the valence and the ionic radius of the solvent cations, Li^+ and Rb^+ in this case[3]. On the other hand, peaks at -1.78 and -2.12 V would be the reduction of iron and chromium ion which would be impurity coming from the dissolution of the sample tube.

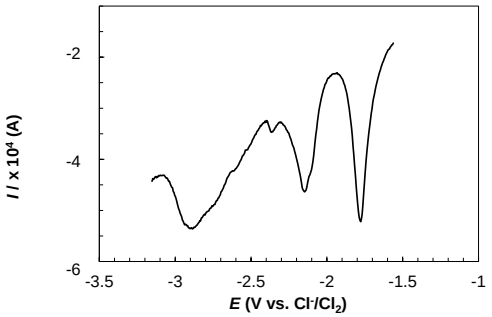

Fig.2 Differential pulse voltammogram of Am in LiCl-RbCl eutectic at 673 K.

REFERENCES:

[1] A. Uehara, *et al.*, J. Nucl. Mater. 414 (2011) 336-339.
[2] M. Iizuka, *et al.*, J. Nucl. Mater. 299 (2001) 32-42.
[3] K. Fukasawa, *et al.*, J. Alloys Compds. 509 (2011) 5112-5118.

採択課題番号 24P2-2　溶融塩及び水和物溶融体中におけるアクチノイドイオンの　プロジェクト分光電気化学的研究

（京大・原子炉）上原章寛、藤井俊行、森山裕丈、山名　元（原子力機構）永井崇之

PR2-3 Effect of Fluoride Addition on UV-vis Spectra of Neodymium Cation in Molten Chlorides

H. Matsuura, K. Fujita, A. Nezu, H. Akatsuka, H. Yamana[1] and T. Fujii[1]

Research Laboratory for Nuclear Reactors, Tokyo Institute of Technology
[1]Research Reactor Institute, Kyoto University

INTRODUCTION: Neodymium is one of the rare earths and it is widely used mainly as a neodymium magnet. The neodymium magnet has the strongest magnetism among the permanent magnets and it has been used as voice coil motors of hard disk drives and motors in hybrid vehicles, electric vehicles, hybrid electric vehicles, wind farms and medical instruments which requires of strong magnetism. The demand of neodymium increases along with increasing the demand of neodymium magnets. However, over 90 % of the first resources of rare earths including neodymium are now in China [1]. Although the price of neodymium tends to decrease recently, the lack of rare earths resources is a concern depending on the strategy of China. Therefore, we have focused on used nickel misch metal hydride batteries as the secondary resource of rare earths, and investigated applicability of molten salt electrolysis to extract neodymium. For the fundamental study, the electron absorption spectra of LiCl-KCl-$NdCl_3$-LiF and NaCl-2CsCl-$NdCl_3$-NaF has been measured to investigate the correlation between the structure and the electrochemical behavior by the addition of fluorides.

EXPERIMENTS: UV-vis spectroscopy of molten salts containing neodymium cation has been carried out by using the spectrophotometer (JASCO V-500) at the hot labo in KURRI [2]. The solvent salts of LiCl-KCl or NaCl-2CsCl was initially molten in a quartz cell (light path: 1cm) installed in the argon circulated glove box and the background absorption spectrum was measured. Then, anhydrous neodymium chloride was added and electronic absorption spectrum of neodymium was obtained by the extraction of the background from the spectrum. In order to look at the effect of fluoride in absorption spectra, LiF (upto 35 times of the molar concentration of neodymium) or NaF (upto 10 times of the molar concentration of neodymium) was added stepwisely to molten LiCl-KCl or NaCl-2CsCl melts, respectively. Before the measurement, the molten salts containing fluoride were well confirmed that the mixtures were homogeneously mixed without any bubbles in the light path.

RESULTS and DISCUSSION: It is well known that the evolution of hypersensitive transition in the electronic absorption of neodymium is related to the indication of the symmetric characteristics of 6 anions octahedral coordinated species around neodymium cation [3]. The electronic absorption spectra of neodymium in molten LiCl-KCl-LiF (Fig.1a) shows that with increasing the concentration of LiF, the main absorption peak is slowly shifted to the lower wavelength and new absorption shoulder appears at ca 575 nm. Contrary to the case of LiCl-KCl-LiF, the electronic absorption spectra in molten NaCl-2CsCl-NaF (Fig.1b) shows much drastic effect depending on fluoride concentration, i.e. molar absoptivity rapidly decreases until the concentration of 6 times to the neodymium and it seems saturated over this concentration. It can be clearly identified that the peak at ca. 575 nm is related the fluoride coodinated species. The reason of the difference of the tendency would be the symmetric characteristics of neodymium species and/or the effect of the coulombic interaction between the cation existing in 2nd coordination sphere (in this case Li^+ or Na^+) from neodymium. EXAFS and Raman spectroscopy should be carried out to elucidate the complicated behaviour of fluoride addition effect before performing numerical calculation study.

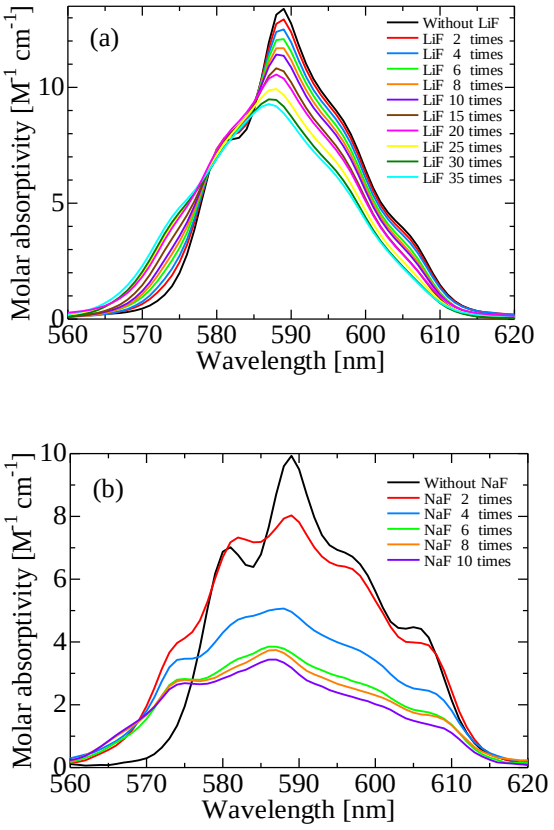

Fig.1 electronic absorption spectra of neodymium in molten (a) LiCl-KCl-LiF and (b) NaCl-2CsCl-NaF.

REFERENCES:

[1] T. Nishiyama: *Rea metaru shigen (rare metal and minerals)*, Maruzen, (2009), 140.
[2] T. Fujii *et al.*, J. Alloys Compd., **393** (2005) L1.
[3] Yu. A. Barbanel *et al*, J. Radioanal. Nucl. Chem., **143** (1990) 167.

採択課題番号 24P2-3アクチニド元素及び FP 元素含有ハロゲン化物の XAFS 構造解析 プロジェクト
（東工大・原子炉研）松浦治明、赤塚　洋、根津　篤
（京大・原子炉）上原章寛、山名　元、藤井俊行

PR2-4 Chemical Isotope Effect of Actinides and Fission Product Elements

T. Fujii, S. Fukutani and H. Yamana

Research Reactor Institute, Kyoto University

INTRODUCTION: Palladium 107 (^{107}Pd) is known as one of long lived fission products. In order to know the nuclear properties of Pd isotopes, Nakamura and co-workers [1] have studied on neutron capture cross section of ^{107}Pd. The isotopic analytical technique is helpful to understand the fractionation mechanism of Pd isotopes in environmental samples and so on. In parallel with the analytical studies, quantum chemical calculations are performed to check the validity of analytical results. The equilibrium constant of the isotope exchange reaction can be theoretically obtained as the reduced partition function ratio (RPFR) of isotopologues. The RPFR value is usually calculated through harmonic vibration analysis. In this study, we report some *ab initio* calculations of hydrated Pd^{2+} complexes.

COMPUTATIONAL DATAILS: The orbital geometries and vibrational frequencies of aqueous Pd(II) species were calculated by using the density functional theory (DFT) as implemented by the Gaussian03 code. The DFT method employed here is a hybrid density functional consisting of Becke's three-parameter non-local hybrid exchange potential (B3) with Lee-Yang-and Parr (LYP) non-local functionals. Similar to an *ab initio* study on aqueous Pd(II) chlorides, we selected the basis sets. The 6-311+G** basis set (all-electron basis set) was chosen for H, O, and Cl. An effective-core potential (ECP) basis set, CEP-121G, was chosen for Pd. The detailed procedure can be seen elsewhere [2].

RESULTS: In order to evaluate the respective strength of mass-dependent effects, we performed some quantum chemical analysis calculations of the vibrational energies of the aqueous Pd(II) species. It is well known that the core structure of Pd(II) complex has the square-planar structure via the hybrid orbital dsp^2. The hydrated Pd^{2+} with the first coordination sphere is generally expressed as $Pd(H_2O)_4^{2+}$. For this equatorial plane, two water molecules are arranged at the axial orientation. The shell including the first coordination sphere and the two water molecules called "meso-shell." The Pd-O bond length for water molecules at the axial positions is longer than that at the equatorial positions. The two waters at the axial position are stabilized by water molecules in second coordination sphere.

Calculation of the aqua complex was examined. We performed structural analysis of $Pd(H_2O)_4^{2+}$ and $Pd(H_2O)_{14}^{2+}$. Our calculation results are consistent with other calculation methods (see [2]). Isotope fractionation of Pd has been found in a chloride system [2]. The acidity dependence of the fractionation [2] should be due to the difference in the vibrational energy of Pd aqua- and chloro- complexes.

Fig. 1. Structure of $Pd(H_2O)_{14}^{2+}$.

The structures of $PdCl_n(H_2O)_{4-n}^{2-n}$ and $PdCl_n(H_2O)_{14-n}^{2-n}$ (n = 0, 1, 2, 3, or 4) were optimized and then intramolecular frequencies of these species were calculated. The isotope enrichment factor due to the intramolecular vibrations can be evaluated from the reduced partition function ratio (RPFR) [3]. It was found that the complexation of Pd^{2+} with Cl^- depress the RPFR value.

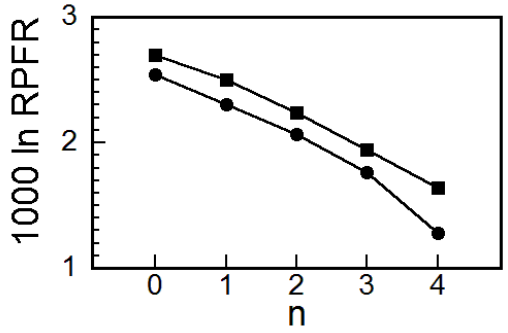

Fig. 2. Reduced partition function ratio (RPFR) of $PdCl_n(H_2O)_{4-n}^{2-n}$ (●) and $PdCl_n(H_2O)_{14-n}^{2-n}$ (■). *n* means number of Cl^- in first coordination sphere of Pd^{2+}.

REFERENCES:

[1] S. Nakamura *et al.*, J. Korean Phys. Soc., 59, 1773 (2011).
[2] T. Fujii *et al*., Proc. Radiochim. Acta 1, 339 (2011).
[3] J. Bigeleisen and M. G. Mayer, J. Chem. Phys. 15, 261 (1947).

採択課題番号 24P2-4　アクチニド元素及び FP 元素の化学同位体効果に関する研究　プロジェクト

（京大・原子炉）藤井俊行、福谷　哲、山名　元

PR2-5 Solvent Extraction of Molybdenum from Hydrochloric Acid with Aliquat 336

T. Yokokita, Y. Kasamatsu, N. Shiohara[1], N. Takahashi, T. Yoshimura[2], K. Takamiya[3] and A. Shinohara

Graduate School of Science, Osaka University
[1]Faculty of Science, Osaka University
[2]Radioisotope Research Center, Osaka University
[3]Research Reactor Institute, Kyoto University

INTRODUCTION: Chemistry researches on heavy-actinide and transactinide elements at the uppermost end of the periodic table are very important in inorganic chemistry. Chemical properties of these elements are expected to be characteristic due to strong relativistic effects on their electronic shells. Chemical experiments of these elements must be carried out on single atom scale, because of their short half-lives and low production rates in the nuclear reactions. It is, therefore, very difficult to perform chemical experiments of these elements. The chemical experiments of the transactinide elements have been performed mainly by simple partition method and detection method is limited to an alpha-particle measurement. In the chemical studies, the complex formation and chemical species of the transactinides were investigated based on the comparison of its chemical behavior with those of lighter homologous elements.

In our previous study, we carried out solvent extraction of molybdenum (Mo) and tungsten (W), which were produced in nuclear reactions and transported by He/KCl gas-jet system, in Aliquat 336/HCl system for chemistry of element 106, seaborgium (Sg) [1]. In this work, we carried out solvent extraction of carrier-free Mo using ^{99}Mo obtained from a Kyoto University Reactor (KUR) multitracer [2].

EXPERIMENTS: The ^{99}Mo was separated from the KUR multitracer by anion-exchange chromatography. Solvent extraction of ^{99}Mo was performed by mixing 1 mL of 2–11 M HCl solution containing ^{99}Mo with 1 mL of 0.011–0.23 M Aliquat 336 chloroform solution in a polypropylene (PP) tube. The mixture was mechanically shaken for 30 min. After centrifuging the solution, the same volumes of both the phases were pipetted in separate PP tubes and then were subjected to γ-ray spectrometry with a Ge semiconductor detector. Distribution ratio (D) was determined from the radioactivity of ^{99}Mo. The D values were determined using the equation:

$$D = A_{org}V_{aq}/A_{aq}V_{org} \quad (1)$$

where A represents the radioactivity and V represents the volume of the solution. The subscripts "aq" and "org" denote the aqueous and organic phases, respectively.

RESULTS: The variations of the D values of Mo as a function of HCl concentration at 0.05 M of Aliquat 336 are shown in Fig. 1. The D values are good agreement with those in Ref. [1] at 8 and 11 M HCl solutions. However, the D values were higher than those in Ref [1] at 2 and 5 M HCl solutions. In the previous experiment with the shaking time of 3 min, chemical reactions in the extraction would not be in equilibrium in lower than 5 M of HCl.

We investigated the relationship between the D value and Aliquat 336 concentration at 11 M of HCl to determine the net charge of the extracted Mo complex. The result is shown in Fig. 2. The linear relationship between log$D$ and log[Aliquat 336] is observed. The slope value of the linear line is 1.0 ± 0.1. The present data indicate that anionic complex of Mo with net charge of −1 would be extracted into Aliquat 336 chloroform solution from 11 M HCl solution. The $[MoO_2Cl_3]^-$ complex can be suggested based on Ref. [3].

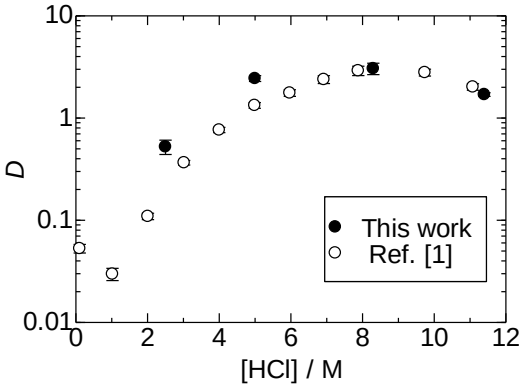

Fig. 1. Variation of the D value of ^{99}Mo as a function of HCl concentration at 0.05 M of Aliquat 336.

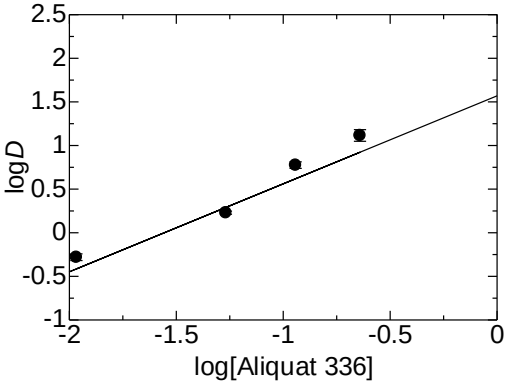

Fig. 2. Variation of the D value of ^{99}Mo as a function of Aliquat 336 concentration at 11 M of HCl.

REFERENCES:

[1] K. Ooe *et al.*, Proc. Radiochim. Acta., **1** (2011) 127-129.
[2] K. Takamiya *et al.*, J. Nucl. Radiochem. Soc., **1** (2000) 81-82.
[3] F. Jaliehvand *et al.*, Inorg. Chem., 46 (2007) 4430-4445.

採択課題番号 24P2-5 重・超アクチノイド元素の化学実験に向けた基礎研究 プロジェクト
（阪大院・理）横北卓也、笠松良崇、高橋成人、篠原 厚（阪大・理）塩原直也（阪大・RI セ）吉村 崇（京大炉）高宮幸一

PR2-6 Measurements of Neutron Capture Cross Sections for Radioactive Nuclei

S. Nakamura, F. Kitatani, T. Fujii[1], A. Uehara[1] and H. Yamana[1]

Japan Atomic Energy Agency
[1]Research Reactor Institute, Kyoto University

INTRODUCTION: A series of experiments with the activation method has been performed to measure thermal-neutron capture cross-sections and resonance integrals of Minor Actinides (MAs), ex. ^{237}Np, ^{244}Cm ^{241}Am and so on. Americium-243 is one of the important MAs, because it has long half-life (7370yr) and products higher Cm isotopes *via* neutron capture reaction, *i.e.* ^{244}Cm, ^{245}Cm, and ^{246}Cm. However, there still exist large discrepancies among reported data of the thermal-neutron capture cross-section (σ_0) as shown in **Fig.1**. This situation might affect the prediction of the amount of product nuclides. This work reports the situation of the measurements and analysis for the neutron capture cross-section of the ^{243}Am(n,γ) reaction.

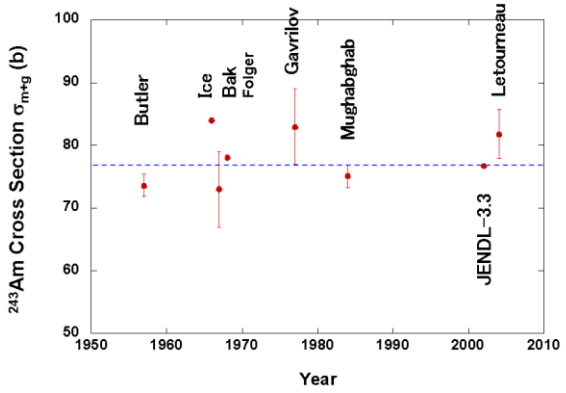

Fig.1 Situation of the reported data for σ_0

EXPERIMENTS: Adequate amount of a high-purity ^{243}Am standardized solution (999Bq) was prepared for an irradiation sample. Its amount was measured with an alpha spectrometer, EG&G ORTEC SOLOIST alpha spectrometer. The irradiation for the ^{243}Am sample was performed for 1 hour at the Pn-2 of the KUR. Pieces of Au/Al and Co/Al alloy wires were irradiated together with the Am sample to monitor neutron flux components at the irradiation position. A high-purity Ge detector was used to measure the γ rays emitted from the Am sample and wires to obtain their induced activities. **Figure 2** shows an example of γ-ray spectrum of ^{243}Am sample. Decay γ rays emitted from ^{244g}Am (10.1h) were observed at the energies of 154, 744 and 898 keV.

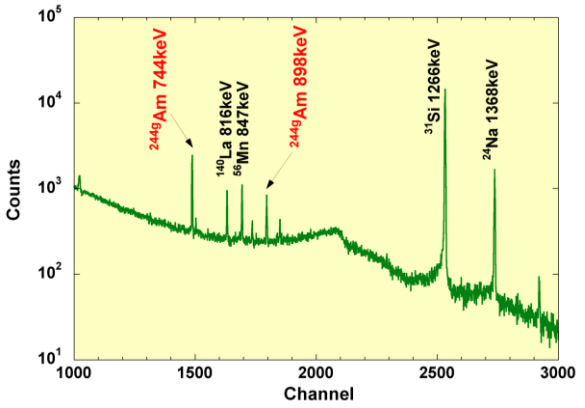

Fig.2 An example of γ-ray spectrum of ^{243}Am sample

ANALYSES: When analyzing the spectral data, there was the problem that the γ-ray emission probabilities have about 30% errors **[1]**. The ^{244}Am ground state decays to the 6^+ state of ^{244}Cm by the probability of 100% via β^- decay**[2]**. There is no transition from the isomer to ground states of ^{244}Am. Using this scheme, emission probabilities could be derived straightforward form the ratios of γ-ray yields for 154, 744 and 898 keV as follows:

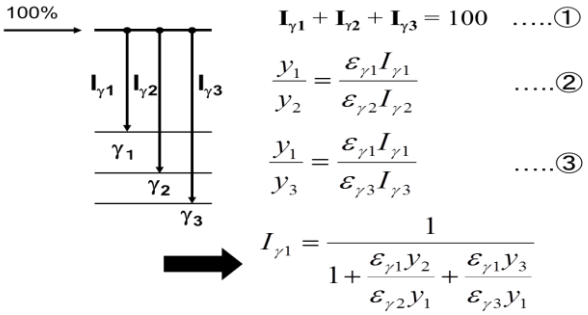

$$I_{\gamma 1} + I_{\gamma 2} + I_{\gamma 3} = 100 \quad \cdots\cdots ①$$

$$\frac{y_1}{y_2} = \frac{\varepsilon_{\gamma 1} I_{\gamma 1}}{\varepsilon_{\gamma 2} I_{\gamma 2}} \quad \cdots\cdots ②$$

$$\frac{y_1}{y_3} = \frac{\varepsilon_{\gamma 1} I_{\gamma 1}}{\varepsilon_{\gamma 3} I_{\gamma 3}} \quad \cdots\cdots ③$$

$$I_{\gamma 1} = \frac{1}{1 + \frac{\varepsilon_{\gamma 1} y_2}{\varepsilon_{\gamma 2} y_1} + \frac{\varepsilon_{\gamma 1} y_3}{\varepsilon_{\gamma 3} y_1}}$$

With this idea, we found the possibility that the emission probabilities of gamma rays would be improved greatly from 30% error to a few %. In this preliminary experiment preliminary, the decay gamma-rays were not followed. In the future experiment, we schedule that the irradiation time is lengthened, and the decay gamma rays are measured enough. It is expected to be able to improve the accuracy of the cross section of ^{243}Am by re-measuring the gamma-ray emission probabilities.

REFERENCES:

[1] R.W.Hoff *et al.*, *Phys. Rev. C*.**29**,618 (1984).
[2] S.E.Vandenbosch *et al.*, *Nucl. Phys.*, **30**,177 (1962).

採択課題番号 24P2-6　　放射化法による長寿命核種の中性子断面積研究　　プロジェクト
（原子力機構）　中村詔司、北谷文人
（京大・原子炉）藤井俊行、上原章寛、山名　元

PR2-7 Elecrochemical Properties of Uranyl Species in 1-Ethyl-3-Methylimidazolium Nitrate

K. Sasaki, M. Harada, T. Suzuki and Y. Ikeda

Research Laboratory for Nuclear Reactors, Tokyo Institute of Technology

(

INTRODUCTION: Room temperature ionic liquids (ILs) are expected to be useful media for recovering uranium from spent nuclear fuels and solid wastes contaminated with uranium [1]. Hence, the extraction behavior of uranyl species from aqueous to IL phase, the electrochemical behavior of uranyl species in ILs, and so on have been studied [2-8]. In the present study, we have examined the structure and electrochemical behavior of uranyl(VI) species in $EMINO_3$ (EMI = 1-ethyl-3-methylimidazoliun).

EXPERIMENTS: $EMINO_3$ and $[EMI]_2[\{UO_2(NO_3)_2\}_2(\mu_4\text{-}C_2O_4)]$ were synthesized based on the reported method [9]. The syntheses of these compounds were confirmed by using NMR and single crystal X-ray analytical methods. Cyclic voltammetry were carried out using BAS ALS model 660B. A three-electrode system was used for preventing the ohmic drop, i.e., a working electrode: glassy carbon, a counter electrode: Pt, a reference electrode: Ag/AgCl (a liquid junction filled with $EMINO_3$).

RESULTS: UV-visible absorption spectrum of $EMINO_3$ solution dissolved $[EMI]_2[\{UO_2(NO_3)_2\}_2(\mu_4\text{-}C_2O_4)]$. The absorption spectrum was found to be similar to that of $DMINO_3$ solution dissolved $[DMI]_2[UO_2(NO_3)_4]$ (DMI = 1.3-dimethylimidazolium). This suggests that the uranyl species in $EMINO_3$ solution dissolved $[EMI]_2[\{UO_2(NO_3)_2\}_2(\mu_4\text{-}C_2O_4)]$ exist as $[UO_2(NO_3)_4]^{2-}$.

Figure 1 shows the cyclic voltammograms of $EMINO_3$ solution dissolving $[EMI]_2[\{UO_2(NO_3)_2\}_2(\mu_4\text{-}C_2O_4)]$ measured at various scan rates (v). As seen from Fig. 1, one reduction and two oxidation peaks are observed at around -0.5 (E_{pc}), -0.3 (E_{pa1}), and 0.03 V (E_{pa2}), respectively, and the peak at around 0.03 V disappear with increasing the scan rate. Furthermore, it was found that the E_{pc} - E_{pa1} values increase with an increase in the scan rate and that the plot of peak currents of E_{pc} *vs.* $v^{1/2}$ gives a linear relationship. From these results, it seems likely that the present reaction proceeds through following mechanism.

$$[U^{VI}O_2(NO_3)_4]^{2-} + e^- \rightarrow [U^{V}O_2(NO_3)_4]^{3-} \quad (E_{pc}).$$

$$2[U^{V}O_2(NO_3)_4]^{3-} \rightarrow [U^{VI}O_2(NO_3)_4]^{2-} + [U^{IV}(NO_3)_n]^{(n-4)-}$$

$$[U^{V}O_2(NO_3)_4]^{3-} \rightarrow [U^{VI}O_2(NO_3)_4]^{2-} + e^- \quad (E_{pa1})$$

$$[U^{IV}O_2(NO_3)_n]^{(n-4)-} \rightarrow [U^{VI}O_2(NO_3)_4]^{2-} + 2e^- \quad (E_{pa2})$$

However, the chemical form of uranyl species in $EMINO_3$ must be examined in more detail.

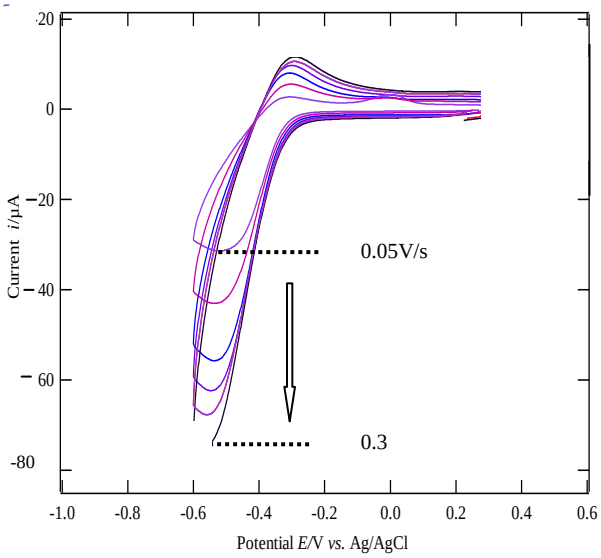

Fig. 1. Cyclic voltammograms of the solution prepared by dissolving $[EMI]_2[\{UO_2(NO_3)_2\}_2(\mu_4\text{-}C_2O_4)]$ (1.01×10^{-2} M) into $EMINO_3$ measured at different scan rates (v = 0.05 ~ 0.3V/s). Initial scan direction: cathodic. Temp. = 65 ºC.

REFERENCES:

[1] V. Cocalia, K. Gutowski, and R. Rogers, *Coord. Chem. Rev.*, **250**, 755 (2006).
[2] K. Binnemans, *Chem. Rev.*, **107**, 2592 (2007).
[3] I. Billard and C. Gaillard, *Radiochim. Acta*, **97**, 355 (2009).
[4] Y. Ikeda, K. Hiroe, N. Asanuma, and A. Shirai, *J. Nucl. Sci.Technol.*, **46**, 158 (2009).
[5] A.-V. Mudring and S. Tang, *Eur. J. Inorg. Chem.*, **2010,** 2569.
[6] T.J. Bell and Y. Ikeda, *Dalton Trans.*, **40**, 10125 (2011).
[7] X. Sun, H. Luo, and S. Dai, *Chem. Rev.*, **112**, 2100 (2012).
[8] P.R. Vasudeva Rao, K. A. Venkatesan, A. Rout, T.G. Srinivasan, and K. Nagarajan, *Sep. Sci. Technol.*, **47**, 204 (2012).
[9]A.E. Bradley, C. Hardacre, *et al.*, *Inorg. Chem.*, **43**, 2503 (2004).

採択課題番号 24P2-7　　f-元素の有効利用に関わる基礎及び応用研究　　プロジェクト
（東工大・原子炉）佐々木琴江、鈴木智也、原田雅幸、池田泰久

PR2-8 Temperature Effect on the Solubility and Solid Phase Stability of Thorium Hydroxide

T. Kobayashi, T. Sasaki and H. Moriyama[1]

Graduate School of Engineering, Kyoto University
[1]Research Reactor Institute, Kyoto University

INTRODUCTION: Safety assessment of geological disposal requires a prediction of solubility limit of tetravalent actinide (An(IV)) over a considerable time-span more than 100 thousands of years. An(IV) is easily hydrolyzed to form amorphous hydroxide ($An(OH)_4$(am)) which controls the solubility limit. However, meta-stable $An(OH)_4$(am) is potentially stabilized to more thermodynamically stable crystalline oxide (AnO_2(cr)) during extremely long period of disposal or under relevant elevated temperature condition in the disposal site. In the present study, we focused on the solubility and solid phase stability of thorium (Th(IV)) hydroxide after heating at 90°C. Th solubility was measured and the solubility product correlated to the particle size of solid phase.

EXPERIMENTS: A Th stock solution diluted to obtain sample solutions, and pH value was adjusted by $HClO_4$/NaOH. The sample solutions were placed into an oven controlled at 90°C and kept for given periods. After aging, the sample solutions cooled down to 25 ºC and the pH values measured. The supernatant was filtered (3k - 100k Da filter, Millipore) and Th concentration determined by ICP-MS (HP4500, Hewlett Packard). The detection limit was about 10^{-8} M. The solid phase was analyzed by X-ray diffraction (XRD) measurement (RINT 2000, RIGAKU).

RESULTS: Fig. 1 shows the Th(IV) solubility after heating at 90 ºC at ionic strength (I) = 0.1, together with the solubility of $Th(OH)_4$(am) kept at 90 and 25 ºC [1,2]. The solubility after heating at 90 ºC for 7days starts to decrease compared to those at 25 ºC, and the values after 41 days are approximately 3 orders of magnitude lower than those of $Th(OH)_4$(am) kept at 25 ºC. Analyzing the solubility data after heating, the solubility product values were determined.

In the XRD spectra of the solid phases, broad peaks corresponding to ThO_2(cr) were observed, indicating the crystallization of the initial $Th(OH)_4$(am). It is note that several sharp peaks (2θ = 30.0, 31.2, 37.2, 39.6, and 47.5 º at I = 2.0) attributed to $NaClO_4$, which was used as back electrolyte. As the peaks 2θ = 27.6, 45.9 and 54.4 º attributed to ThO_2(cr) and the particle size (D) of solid phase was calculated using Scherrer equation:

$$D = K\lambda / \beta \cos\theta \qquad (1),$$

where K, λ, β, and θ represent Scherrer constant, X-ray wavelength (Cu-Kα), the line broadening at the half maximum intensity (FWHM) in radian, and the Bragg angle.

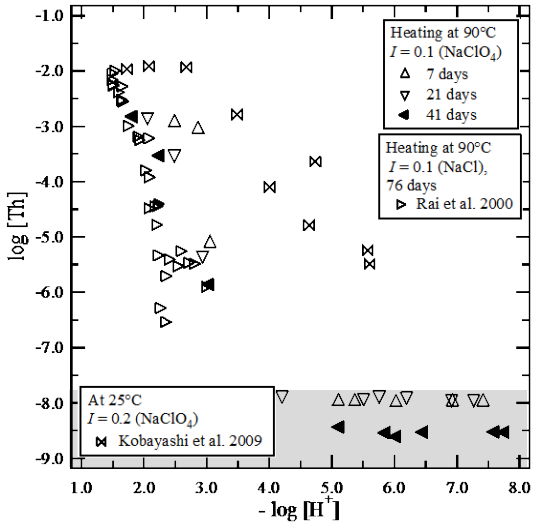

Fig. 1 Th solubilty after heating at 90 ºC (3kDa)

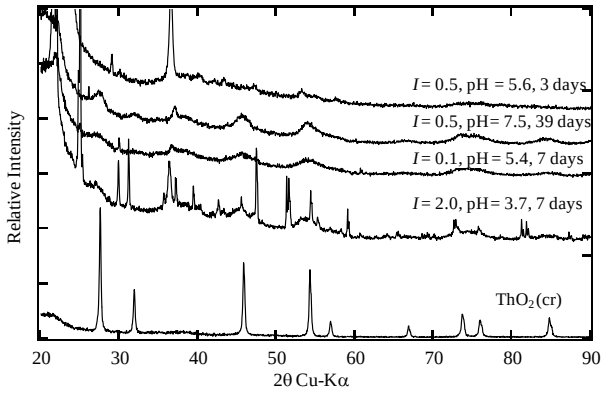

Fig. 2 XRD spectra of Th solid phase after heating at 90 ºC

The relationship between obtained solubility product value and particle size of the solid phase after heating are in agreement with the Schindler equation [3], where the solubility product decreases with increasing particle size. This work exemplifies the predicted transformation of amorphous phase into a thermodynamically more stable phase, and therefore less soluble solid of higher crystallinity. This finding adds highlight to understand an important mechanism relevant for predicting actinide solubility at repository conditions.

REFERENCES:

[1] Rai *et al.* Radiochim. Acta **88**, (2000) 297.
[2] Kobayashi *et al.* J. Nucl. Sci. Technol. **46**, (2009)1085.
[3] Schindler, P. W., Adv. Chem. Ser., **67**, (1967) 196.

採択課題番号 24P2-8　アクチニド元素の水溶液内錯生成反応に関する研究　　プロジェクト
（京大院・工）佐々木　隆之、小林　大志、上田　健揚、伊達　海斗、松浦　由佳、上村　拓也（京大・原子炉）藤井　俊行、山名　元

PR2-9 Reduction Behavior of UCl_3 on Ni and Al Electrodes in LiCl-KCl Eutectic Melt at 773 K

Y. Sakamura, M. Iizuka, K. Uozumi, T. Fujii[1], A. Uehara[1] and H. Yamana[1]

Central Research Institute of Electric Power Industry
[1]Research Reactor Institute, Kyoto University

INTRODUCTION: Electrorefining process using molten chloride salt bath is under development worldwide for nuclear fuel cycle. Actinides contained in spent nuclear fuels are dissolved into the salt at the anode, and then are collected at the cathode. Liquid Cd cathode is employed to collect Pu together with U and minor actinides (Np, Am and Cm). Because of chemical similarity, some of rare earth fission products are also deposited in the Cd cathode. Since Ni and Al form intermetallic compounds with actinides, they are expected to be an alternative for the cathode material to enhance the separation factor between the actinides and rare earths. The Ni cathode has been studied to separate Dy from Nd contained in used Nd magnets [1], and the Al cathode has been studied for the electrorefining process of spent nuclear fuels [2]. In this study, reduction behavior of UCl_3 on Ni and Al electrodes in LiCl-KCl eutectic salt bath are investigated by cyclic voltammetry.

EXPERIMENTS: LiCl-KCl eutectic melt was contained by a high-purity alumina crucible at 773 K, where a working electrode of Ni, Al or W wire (1 mm diameter), a counter electrode of glassy carbon rod (3 mm diameter), a Ag/AgCl reference electrode and a type-K thermocouple were placed. The W wire was employed as the inert electrode because W metal does not form any alloys with U or Li metal. The Ag/AgCl electrode consisted of a Ag wire immersed in a LiCl-KCl eutectic salt mixture with 1 wt% AgCl, which was contained in a closed-end Pyrex tube. The potential used in this paper is relative to the Ag/AgCl potential, unless otherwise stated. The potential of the Ag/AgCl electrode was 2.407 V against a Li metal electrodeposited on a Ni wire. The concentration of UCl_3 was incrementally changed by adding a prepared LiCl-KCl-UCl_3 salt whose U concentration was 11.4 wt% determined by ICP-AES analysis. All the measurements were conducted in a high-purity Ar atmosphere glove box (H_2O, O_2 < 1 ppm).

RESULTS: The blank test was conducted in a LiCl-KCl eutectic alone. The cyclic voltammogram (CV) of Al has a cathodic current peak rising at about -1.9 V, which should correspond to the formation of Li-Al alloy. As for the CVs of Ni and W, no cathodic current is observed in the potential range more positive than -2.4 V where Li metal is deposited.

Figure 1 shows typical CVs of the Ni, Al and W electrodes in a LiCl-KCl-UCl_3 (0.16 mol%) melt. The working electrode potential was first scanned from the rest potential to -1.6 V and then was reversely scanned. The CV of W indicates that reduction of U^{3+} to U metal occurred by a one-step process for the reduction wave at -1.45 V, followed by reoxidation of the deposited U metal at the electrode surface during the anodic sweep.

On the Ni electrode, a small cathodic current corresponding to the formation of U-Ni alloys rises from -1.25 V. In addition to the anodic peak for reoxidation of the deposited U metal, there are several anodic peaks, which indicates that U dissolves from the different U-Ni alloys. Several alloys (UNi_6, UNi_2, U_5Ni_7, U_7Ni_9 and U_6Ni) are shown in the phase diagram of U-Ni system [3]. Besides, two anodic currents located at around 0.2 V and 0.0 V should correspond to the U^{3+}/U^{4+} and Ni/Ni^{2+} couples, respectively. It is noted that the anodic peaks for oxidation of the U-Ni alloys are much smaller than that of the pure U metal. Hence, the formation reaction of U-Ni alloys is relatively slow compared with the rare earth-Ni systems [1].

The rest potential of the Al electrode, around -1.03 V, is more negative than those of the Ni and W. In the CV of Al, the cathodic current rises from the rest potential, which is attributed to the formation of U-Al alloys [2]. The cathodic current peak for pure U metal deposition is also observed at -1.45 V. It is indicated that the formation reaction of U-Al alloys is faster than that of U-Ni alloys. The anodic current rising steeply from -1.03 V should be due to the dissolution of U and Al from the U-Al alloys. Therefore, it is suggested that U cannot be separated from Al by the anodic dissolution of U-Al alloys.

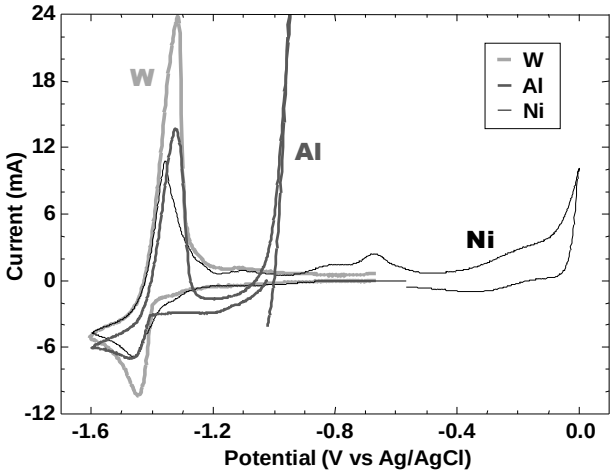

Fig. 1 CVs of W (ϕ1 x 5 mm), Al (ϕ1 x 7 mm), and Ni (ϕ1 x 5 mm) wire electrodes in LiCl-KCl eutectic melt containing 0.16 mol% of UCl_3 at 773K. Scan rate 0.1 V/s.

REFERENCES:

[1] H. Konishi *et al.*, *Molten Salts*, **54**(1), 21 (2011) [in Japanese]
[2] P. Soucek *et al.*, *Proc. Int. Conf. Global 2009*, pp. 1156, Paris, France, Sept. 6-11, 2009.
[3] T. B. Massalski, *Binary Alloy Phase Diagrams*, Vol. 2, American Society for Metals, Metals Park, OH, 1986

採択課題番号 24P2-9　溶融塩化物中でのウランの酸化還元挙動に関する乾式再処理基礎研究　プロジェクト

（電中研）坂村義治、飯塚政利、魚住浩一（京大・原子炉）山名　元、藤井俊之、上原章寛

PR2-10 Electrochemical Behavior of f-Elements Compound

T. Goto and K. Hachiya[1]

Department of Environmental Systems Science, Faculty of Science and Engineering, Doshisha University
[1]Department of Fundamental Energy Science, Graduate School of Energy Science, Kyoto University

INTRODUCTION: Molten salts are promising media for separation and recovery of the spent nuclear fuel. To realize the process, clarifying the physicochemical properties of FP elements in molten salts is required. Although cesium is known as an important fission product, little has been reported about its effect on the molten salts. From the background, we have examined the influence that the existence of the cesium ion gave to other multi valence ions in molten LiCl-KCl. In this report, aluminum ion was selected as model of a multi valence cation and electrochemical behavior and liquid structures of molten alkaline chlorides containing Al were investigated.

EXPERIMENTS: The LiCl-KCl-CsCl eutectic (LiCl-KCl-CsCl=57.5:13.3:29.2 mol %) was used as an electrolyte for electrochemical measurement. $AlCl_3$ was directly added to the melt as an Al(Ⅲ) source. All experiments were conducted in an argon atmosphere with a continuous gas refining instrument. A tungsten wire electrode covered with a high purity alumina tube was used as a working electrode for investigating electrochemical behavior of aluminum ions. Diffusion coefficient of aluminum ions was determined by means of electrochemical measurement. Raman scattering spectra were obtained for $AlCl_3$, LiCl-KCl eutectic melt +3mol% $AlCl_3$, LiCl-KCl-CsCl eutectic melt + 3 mol% $AlCl_3$, NaCl-$AlCl_3$ 1:1 melt. Simulated Raman spectra were also attained through density-functional-theory calculations with GAUSSIAN 09.

RESULTS: Diffusion coefficient of Al(Ⅲ) in LiCl-KCl-CsCl at 603 K was determined to be 4.0×10^{-8} $cm^2\ s^{-1}$. The diffusion coefficient was 3 orders lower than that in LiCl-KCl. This implied the coordination of aluminum ion in the molten salts was affected by the existence of the cesium ion. Raman spectroscopy was carried out to characterize the melt structures. Experimental and calculated Raman spectra are given in Figs. 1 and 2. A hybrid functional, B3LYP, was used for exchange-correlation functional, and 6-311G**, 6-311++G**, and aug-cc-pVTZ were used for basis functions. Finite-temperature liquid structure was also analyzed through atom-centered density matrix propagation (ADMP) simulation, a variant of ab-initio molecular dynamics simulations, with split valence basis function of m-def2-SVP and HSEh1PBE hybrid correlation-exchange functional for 1:1 CsCl-$AlCl_3$ mixture at 700 K. As have been reported and discussed [1], $AlCl_4^-$ cluster structure is expected for anion in basic and neutral molten aluminum–alkaline-metal chloride mixtures. Our calculation basically confirmed the dominance of $AlCl_4^-$ at neutral condition, but transient existence of $Al_2Cl_7^-$ was also observed as have been reported for other aluminum–alkaline-metal chloride melts [2].

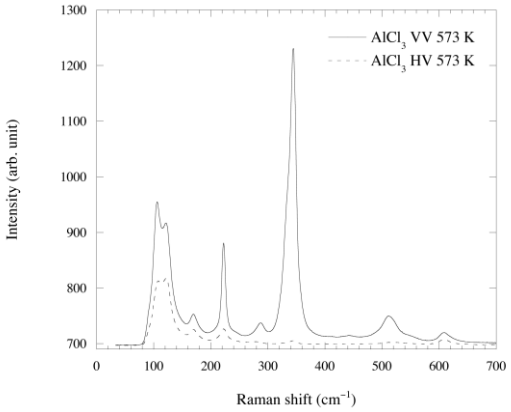

Fig. 1 Raman scattering spectra for molten $AlCl_3$ at 573 K.

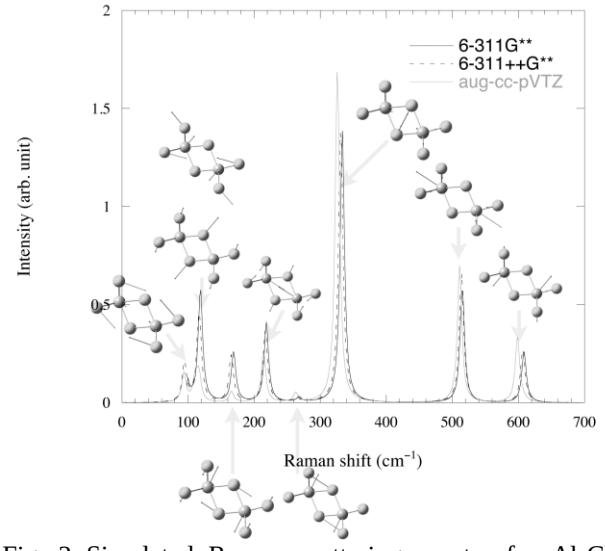

Fig. 2 Simulated Raman scattering spectra for Al_2Cl_6 cluster.

REFERENCES:

[1] M. P. Tosi, D. L. Price, M.-L. Saboungi, Annu. Rev. Phys. Chem., 44, 173 (1993).
[2] M. Salanne, L. J. A. Siqueira, A. P. Seitsonen, P. A. Madden, B. Kirchner, Faraday Discuss., 154, pp. 171-188 (2012).

採択課題番号 24P2−10　　溶融塩中における f−元素化合物の電気化学的形成・溶解に関する基礎研究　　プロジェクト
（同志社大・理工）後藤琢也（京大院・エネ科）蜂谷　寛

PR2-11

Characterization of Neodymium Ion in Molten $CaCl_2$ in Equilibrium with Neodymium Triborate, NdB_3O_6

H. Sekimoto, A. Uehara[1], T. Fujii[1] and H. Yamana[1]

Department of Materials Science and Engineering, Faculty of Engineering, Iwate University
[1]Research Reactor Institute, Kyoto University

INTRODUCTION: Development of recycling technique for neodymium magnet is essentially important to achieve sustainable society. Consequently, we propose and are investigating a new recycling process of neodymium magnet shown in Fig. 1. In the proposed process, the neodymium magnet is melted together with sufficient amount of B_2O_3 in graphite crucible to form molten iron based alloy and Nd_2O_3-B_2O_3 slag, which is recovered and dissolved in molten salt. And then, Fe-Nd-B alloy is produced by molten salt electrolysis. In this study, as the first stage of the research on the molten salt electrolysis in the proposal, we investigated the dissolution behavior of neodymium triborate, NdB_3O_6, which is the main component of recovered Nd_2O_3-B_2O_3 using absorption spectroscopy.

EXPERIMENTS: The absorbance of $CaCl_2$ molten containing a given amount of dissolved $NdCl_3$ at 800 °C was measured to obtain the absorption spectrum of trivalent neodymium ion. And then, we measured the absorption spectrum of trivalent neodymium ion in $CaCl_2$ molten salt in equilibrium with the mixture of NdB_3O_6 and B_2O_3 which is prepared by melting 5.7 g of Nd_2O_3 and 4.3 g of B_2O_3 in graphite crucible at 1200 °C.

RESULTS: Figure 2 shows the absorption spectra of trivalent neodymium ion in $CaCl_2$ molten salt at 800 °C. The broken lines were obtained as the results of the measurement of the absorbance of $NdCl_3$ dissolved in $CaCl_2$ molten salt. The spectra are similar to the absorption spectra of neodymium chloro complex ion in LiCl-KCl eutectic molten salt at 600 °C obtained by Fujii *et al.* [1] On the other hand, the solid line corresponds absorption spectrum of the neodymium ion in equilibrium with the mixture of NdB_3O_6 and B_2O_3 and $NdCl_3$. The shape of the spectrum is the same as the spectra of chloro complex ion obtained by the measurement of the absorbance of $NdCl_3$ dissolved in $CaCl_2$ molten salt. This result indicates that the neodymium ion in NdB_3O_6 dissolved in $CaCl_2$ molten salt as chloro complex ion. Supposing that NdB_3O_6 is the mixture of Nd_2O_3 and B_2O_3 (where the molar ratio of Nd_2O_3 to B_2O_3 is 1/3), the dissolution reaction of neodymium ion in $CaCl_2$ from NdB_3O_6 is considered to be represented by the following reaction,

$$Nd_2O_3 \text{ in } NdB_3O_6 + 3CaCl_2 \rightarrow 2NdCl_3 + 3CaO \ . \quad (1)$$

We then estimated the concentration of neodymium ion in equilibrium with NdB_3O_6 using the absorption spectra. The calibration curve of the concentration of neodymium ion was prepared using the absorbance at 590 nm. Using the calibration curve, the concentration of neodymium ion in equilibrium with the mixture of NdB_3O_6 and B_2O_3 at 800 °C was estimated to be 0.3 ± 0.1 mol kg^{-1} in molality.

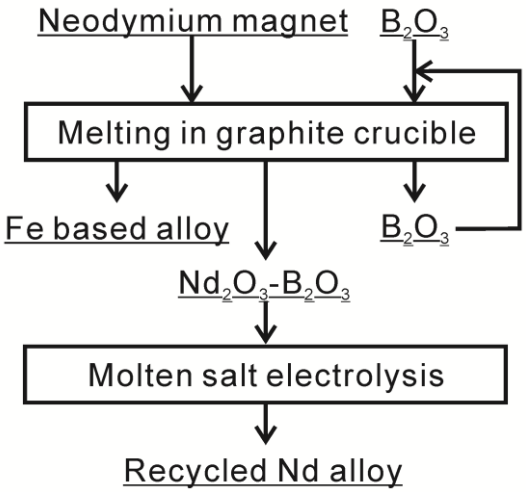

Fig. 1. Flowchart of the recycling process for neodymium magnet proposed in this study.

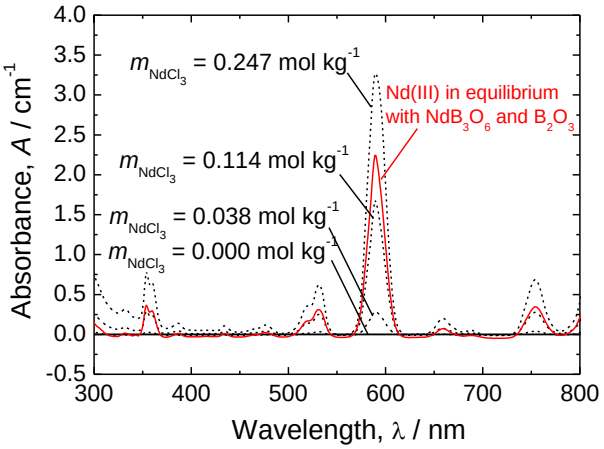

Fig. 2. Absorption spectra of trivalent neodymium ion in $CaCl_2$ molten salt at 800 °C.

REFERENCES:

[1] T. Fujii, H. Moriyama and H. Yamana, *J. Alloy. Compd.*, **351** (2003) L6-L9.

採択課題番号 24P2-11　　吸収分光測定を用いた高温融体中の金属イオンの溶存形態に関する研究　　プロジェクト

（岩手大・工）関本英弘　（京大原子炉）上原　章寛、藤井　俊行、山名　元

PR2-12 Thermal and Mechanical Properties of Actinides-Containing Ceramics - Synthesis of Y_6UO_{12} -

S. Yamanaka, Y. Ohishi, H. Muta and K. Kurosaki

Graduate School of Engineering, Osaka University

INTRODUCTION: The ceramic nuclear waste form has been considered as one of the methods to immobilize actinide elements extracted from high-level radioactive nuclear wastes. Among them, in recent years Y_6AnO_{12} and Yb_6AnO_{12} where *An* represents actinide elements have received attention as appropriate ceramics in which actinide elements can be immobilized stably. When utilizing such ceramics as the waste form, the physical and chemical properties should be understood. However the properties of Y_6AnO_{12} and Yb_6AnO_{12} have been scarcely reported. Previously, our group has investigated the thermal properties of Y_6WO_{12} and Yb_6WO_{12} [1] because Y_6WO_{12} and Yb_6WO_{12} take the same hexagonal crystal structure as that of Y_6AnO_{12} and Yb_6AnO_{12} [2].In the present study, polycrystalline samples of Y_6UO_{12} were synthesized by solid state reactions.

EXPERIMENTS: Y_6UO_{12} was prepared from the mixtures of Y_2O_3 and U_3O_8 by standard solid-state reactions. U_3O_8 was prepared by heating UO_2 in flowing air at 873 K for 6 h. Dried Y_2O_3 powders (Kishida Chemical Co., 99.99%) and U_3O_8 powders were weighed in the appropriate molar ratio and mixed thoroughly in an agate mortar. These oxide mixtures were pressed into pellets at 150 MPa for 5 min at room temperature. The green pellets were then heated in air on an alumina crucible for 24 h at 1673 K. The crystal structure of the samples was analyzed by powder X-ray diffraction (XRD) using Cu-Kα radiation. The microstructure and the element distribution of the samples were analyzed by the scanning electron microscopy (SEM) and the energy dispersive X-ray (EDX) analysis at room temperature.

RESULTS: Figure 1 shows the XRD pattern of the Y_6UO_{12} sample, together with the peak positions reported in the literature. In the XRD pattern, there were no peaks derived from impurities. As shown in Fig. 2, the SEM images revealed that the surface of the Y_6UO_{12} sample was homogeneous with no secondary impurity phases. The quantitative EDX analyses confirmed that the chemical compositions did not deviate a lot from the starting compositions. These results indicate that the single phase material was synthesized in the present study.

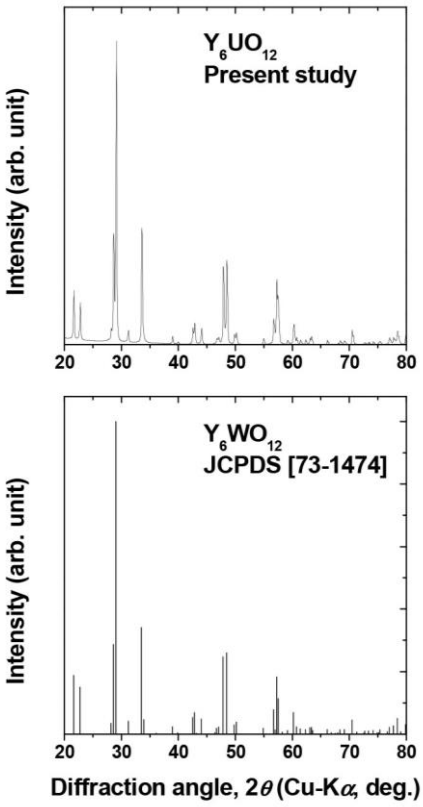

Fig.1 XRD pattern of Y_6UO_{12} sample, together with the peak positions reported in the literature.

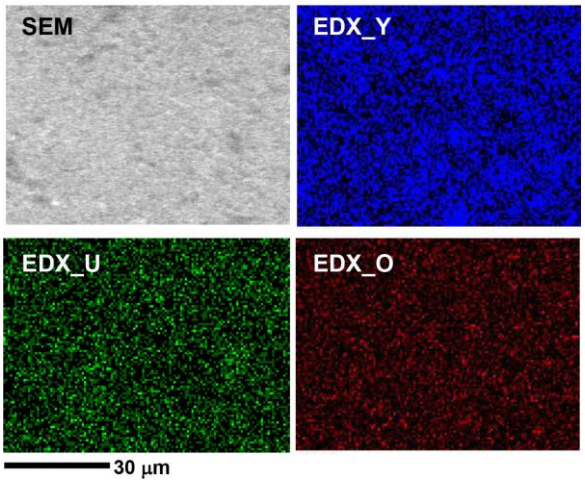

Fig.2 SEM and EDX images of Y_6UO_{12} sample.

REFERENCES

[1] Y. Zheng et al., "Thermal conductivity of Y_6WO_{12}, and Yb_6WO_{12} ceramics," *J. Nucl. Mater.*, **419**, 357-360 (2011).

[2] S. F. Bartram, "Crystal structure of the rhombohedral $MO_3R_2O_3$ compouds (M = U, W, or Mo) and their relation to ordered R_7O_{12} phases," *Inorg. Chem.*, **5**, 749-751 (1966).

採択課題番号 24P2-12　　アクチニド含有酸化物の物性に関する基礎研究　　プロジェクト
（阪大・工）山中伸介、黒崎　健、牟田浩明、大石佑治